THE JOURNAL OF PHYSICAL CHEMISTRY B

Article

pubs.acs.org/JPCB

Recycling of Uranyl from Contaminated Water

Klemen Bohinc,[†,*] Jurij Reščič,[‡] Jean-Francois Dufreche,[§] and Leo Lue[∥]

[†]Faculty of Health Sciences, University of Ljubljana, Zdravstvena 5, SI-1000 Ljubljana, Slovenia

[‡]Faculty of Chemistry and Chemical Technology, University of Ljubljana, Aškerčeva 5, SI-1000 Ljubljana, Slovenia

[§]Institut de Chimie Separative de Marcoule, Universite de Montpellier, 30207 Bagnols sur Ceze Cedex, France

[∥]Department of Chemical and Process Engineering, James Weir Building, University of Strathclyde, 75 Montrose Street, Glasgow G1 1XJ, United Kingdom

ABSTRACT: Many separation processes are related to the behavior of ions close to charged surfaces. In this work, we examine uranyl ions, which can be considered as rod-like molecular ions with a spatially distributed charge, embedded in a system of like charged surfaces. The analysis of the system is based on an approximate field theory which is accurate from the weak to the strong electrostatic coupling regimes. The numerical results show that close to the charged surface the ions are oriented parallel to the surface, whereas at distances greater than half of the ion length, they are randomly oriented. Due to the restriction of the orientational degrees of freedom, the density of ions at the charged surface decreases to zero. For large surface charge densities, the force between like charged surfaces becomes attractive, as a result of charge correlations. The theoretical results are in good agreement with Monte Carlo simulation results.

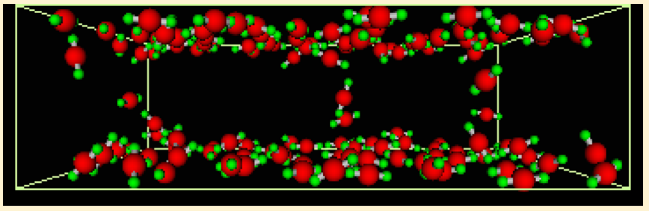

1. INTRODUCTION

Recycling of metallic elements requires the development of complex separation methods. In most of these methods, the metals are in an ionic form. For example, in the case of liquid−liquid extraction, ions are separated thanks to a selective transfer from an aqueous phase[1,2] to an organized organic phase. Thus the understanding of the ion specificity (i.e., the differences between the various ions) for bulk and interfacial geometries is especially important for the design of new separation methods. Small differences in the free energy change can lead to significant changes in the efficiency of the separation process.

Most separation processes for element recovery are based on the behavior of hydrated ions close to an interface,[3] and consequently, interfacial properties have proven to be important. Despite the significance of these methods for the recycling of rare earth metals, the mechanism of the process is far from being well understood. The role of the various physical and chemical effects is not very well understood, and the molecular nature of the ions is most likely an important parameter. Molecular ions, where the charge is spatially distributed[1,4,5] among different sites, occur in many important applications.

In the context of the nuclear fuel cycle, the PUREX process allows the recovery and recycling of major actinides. It makes use of the remarkable properties of an organic molecule, tributyl phosphate (TBP), in term of selectivity for the various elements. Uranium is extracted as the molecular uranyl ion UO_2^{2+},[6] schematically represented in Figure 1. Another important aspect is the adsorption of uranyl ions at the mineral−water interface.[7] The distribution constant is an important quantity for nuclear waste repository and for the remediation of contaminated sites. Further, the distribution of uranyl ions at a charged surface is a very important parameter. The sorption has been studied both experimentally and theoretically.[8] In the case of kaolinite clays[9] and goethite,[10] uranyl ions are oriented parallel to the surface in an inner sphere complex. Classical molecular dynamics simulations[11,12] for montmorillonite clays exhibited outer-sphere complexes with the axis of the uranyl ion tilted at approximately 45° to the surface. The adsorption appears to be dependent on the counterion type.[3] The description of uranyl sorption on mineral surfaces at large distances has also been studied from

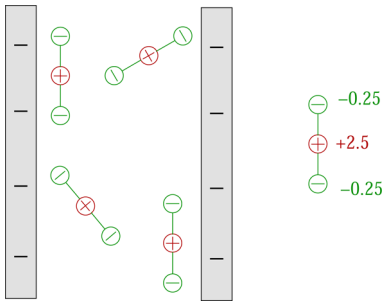

Figure 1. Schematic illustration of the system. The red spheres on the uranyl ion represent uranium ions with charge $+2.5e_0$, whereas the green spheres represent oxygen ions with charge $-0.25e_0$. The uranyl ion has a linear structure with an overall length of 0.36 nm.

Received: May 16, 2013
Revised: August 4, 2013
Published: August 16, 2013

macroscopic ion-exchange and surface complexation modeling such as the ones based on the multisite-complexation (MUSIC) model.[13−15] In that case, ion sorption is taken into account from chemical equilibria at the surface coupled to macroscopic Gouy−Chapman (or Poisson−Boltzmann) equations. The molecular nature of the ion is completely ignored.

Uranyl can be considered to be a rod-like molecular ion with charges distributed along its length. These spatially distributed charges introduce additional intramolecular correlations which need to be considered in addition to the intermolecular Columbic correlations. Through models including ionic correlations, it is possible to explain phenomena not accessible by the analytical theories referred. For instance, overcharging has been a well-known phenomenon reported by experimentalists for small multivalent ions for a long time but excluded from the classical framework. Its relationship with ionic correlations was later recognized providing a reasonable description of this phenomenon.

The study of uranyl ions can be connected to our previous work for rod-like ions. Recently, we demonstrated that intraionic correlations induced by the fixed distance between charges within a particular rod-like ion can be sufficient to change repulsive into attractive interactions between like-charged surfaces.[16,17] The minimum of the free energy occurs when the counterions are oriented perpendicularly to the like-charged surfaces, thus connecting them.[18] This effect of bridging[19] is the structural motif that leads to attraction and eventually to a finite equilibrium distance between two like-charged surfaces. These theoretical predictions are confirmed by Monte Carlo simulations.[20,21] The theory was also generalized to systems with polydisperse rod lengths and arbitrary charge distributions along the rods.[22,23] The addition of monovalent point-like salt ions can turn the attraction between the plates to a repulsive interaction due to screening.[18] The hydration shell around the ions with spatially extended charge was introduced. The first attempt has been made by introducing spheroidal ions with two charges embedded in a spherical structure.[24,25] The model has been extended to ions with a smooth charge distribution on the spherical surface.[26]

While these mean-field theories were able to successfully describe the influence of extended charge distributions on the interaction between weakly charged plates, these theories breakdown as the charge densities of the plates increases. In addition, as the rod-like counterions becomes more compact, it approaches a point-like multivalent ion. In these situations, the charge−charge correlations between counterions becomes important, and the mean field theories also fail to adequately describe these systems. These interionic correlations alone can lead to an attraction between the like-charged surfaces and have attracted considerable interest in the past.[27−30] In the limit where the electrostatic coupling is extremely strong, an expansion has been developed[29,31] which works quite well; however, the conditions where this expansion is valid are more extreme than is typically observed experimentally.

Coalson and Duncan utilized a lattice field theory and calculated the free energy of a system of fixed charged macroions surrounded by mobile ions.[32] They showed that the leading term in the functional integral evaluated at saddle point leads to the mean-field Poisson−Boltzmann equation. The mean field approximation can be systematically corrected by evaluating fluctuations around the saddle point. The lattice field theory approach was later generalized to include the finite size of the simple mobile ions,[33] mobile dipoles and charged polymer chains.[34,35]

A field theoretic approach was recently developed that can properly describe the properties of charged systems from the weak to the intermediate and the strong coupling regimes.[36−38] This theory gives predictions that are in good agreement with computer simulation and has been extended to dimer[39] and rod-like counterions.[37,40,41] In the present work, we use this theory to examine the behavior of molecular uranyl ions between charged surfaces.

The remainder of this paper is organized as follows. First, we formulate a field theoretical description for uranyl, considered as point-like charges distributed along a infinitely thin rod. The system is confined between two like-charged, planar surfaces. In the field theoretic approach, the correlations between different molecules, as well as correlations within a particular molecule are taken into account. Next, the details are provided of the Monte Carlo simulations we performed to test the theory. Then, we make a detailed analysis of weak and strong coupling limits. The resulting integral differential equation is solved numerically. The relevant physical quantities such as the electrostatic potential, the ion distributions, and the free energy are calculated in order to investigate the origin of the selectivity in the separation processes. The pressure between the charged interfaces, which controls the geometry of the system, will also be investigated. Finally, the main findings of this work are summarized, as well as directions for future work.

2. THEORY

The system we consider is schematically represented in Figure 1 and is composed of two like-charged surfaces immersed in an aqueous solution of uranyl ions. Water is treated as a continuum solvent with uniform dielectric constant ε. The uranyl ions are represented as rod-like molecules with a length of l = 0.36 nm and three point charges. In the middle of the rod, the charge of the uranium atom is $q_1 = +2.5e_0$ (where e_0 is the fundamental unit of charge), whereas the charge of the oxygen atoms at both ends of the rod is $q_2 = -0.25e_0$. The charge density $Q(\mathbf{r},\hat{\mathbf{n}})$ of a rod with one end located at $\mathbf{r}$ and the other end located at $\mathbf{r} + l\hat{\mathbf{n}}$, where $\hat{\mathbf{n}}$ is a unit vector, is given by

$$Q(\mathbf{r}, \hat{\mathbf{n}}) = q_1\delta^d(\mathbf{r} - l\hat{\mathbf{n}}/2) + q_2[\delta^d(\mathbf{r}) + \delta^d(\mathbf{r} - l\hat{\mathbf{n}})] \quad (1)$$

The total charge density $Q(\mathbf{r})$ in the system is

$$Q(\mathbf{r}) = \sum(\mathbf{r}) + q(\mathbf{r}) \quad (2)$$

where $\Sigma(\mathbf{r})$ is distribution of fixed charges in the system (i.e., $\Sigma(\mathbf{r}) = \Sigma\delta(z) + \Sigma\delta(z - D)$, where Σ is the surface charge density of the plates and D is the distance between the plates) and $q(\mathbf{r})$ is the charge density due to a collection of N charged rods

$$q(\mathbf{r}) = \sum_{k=1}^{N} Q(\mathbf{r} - \mathbf{R}_k, \hat{\mathbf{n}}_k) \quad (3)$$

where $\mathbf{R}_k$ and $\hat{\mathbf{n}}_k$ are the position and orientation, respectively, of rod k. The fixed charge on both surfaces is neutralized by the charge of uranyl ions.

The electrostatic interactions are the only interactions between the ions in the system; steric effects and other interactions between ions are not considered. The electrostatic interaction energy E can be written as

$$E = \frac{1}{2}\int d\mathbf{r}\, d\mathbf{r}'\, Q(\mathbf{r})G(\mathbf{r},\mathbf{r}')Q(\mathbf{r}) - \sum_{k=1}^{N} e^{se}(\mathbf{R}_k, \hat{\mathbf{n}}_k) \quad (4)$$

where $G(\mathbf{r},\mathbf{r}') = \varepsilon^{-1}|\mathbf{r} - \mathbf{r}'|^{-1}$ is the Green's function of the Poisson equation, which represents the interaction energy between the charges located at $\mathbf{r}$ and $\mathbf{r}'$. The last term in eq 4 $e^{se}(\mathbf{R},\hat{\mathbf{n}})$ represents the self-energy of the uranyl molecules with the electric field generated by its own charge. It is given by

$$e^{se}(\mathbf{R}, \hat{\mathbf{n}}) = \frac{1}{2}\int d\mathbf{r}\, d\mathbf{r}'\, Q(\mathbf{r} - \mathbf{R}, \hat{\mathbf{n}})G(\mathbf{r}, \mathbf{r}')Q(\mathbf{r}' - \mathbf{R}, \hat{\mathbf{n}}) \quad (5)$$

In the following we split the Green's function of the electrostatic interactions into short- and long-wavelength components[36,38]

$$G(\mathbf{r}, \mathbf{r}') = G_s(\mathbf{r}, \mathbf{r}') + G_l(\mathbf{r}, \mathbf{r}') \quad (6)$$

The long and short-wavelength components are given by equations $G_l = \mathcal{P}G$, $G_s = (1 - \mathcal{P})G$, respectively. The operator $\mathcal{P}$ projects out of the full Green's function the long- and short-wavelength components. Here, we choose $\mathcal{P} = [1 - \sigma^2\nabla^2 + \sigma^4\nabla^4]^{-1}$, where the parameter σ is a length scale which separates between long- and long-wavelength fluctuations. This parameter corresponds to the size of the correlation hole around each of the charges.

Using the Hubbard–Stratonovich transformation[42,43] for both the short-wavelength and long-wavelength electrostatic interactions in the system, the grand partition function of the system can be re-expressed as a functional integral over two fields, ψ_s (associated with G_s) and ψ_l (associated with G_l), respectively. The resulting functional integration over ψ_s is evaluated by a first-order cumulant expansion, while the functional integration over ψ_l is evaluated using the mean-field approximation. Details of this procedure can be found in refs 36 and 38 for point charges, ref 39 for dimers, and ref 37 for rod-like counterions.

This leads directly to the following approximate expression for the Helmholtz free energy F of the system

$$\beta F[\rho, \Sigma] \approx \int d\mathbf{R}\, d\hat{\mathbf{n}}\, \rho(\mathbf{R}, \hat{\mathbf{n}})[\ln \rho(\mathbf{R}, \hat{\mathbf{n}})\Lambda^3 - 1] - \frac{1}{8\pi}\int d\mathbf{r}\, \nabla\phi(\mathbf{r})\cdot\nabla i\bar{\psi}_l(\mathbf{r}) + \int d\mathbf{r}\, [\sum(\mathbf{r}) + \int d\mathbf{R}\, d\hat{\mathbf{n}}\, \rho(\mathbf{R}, \hat{\mathbf{n}})Q(\mathbf{r} - \mathbf{R}, \hat{n})] + \int d\mathbf{R}\, d\hat{\mathbf{n}}\, \rho(\mathbf{R}, \hat{\mathbf{n}})\beta u(\mathbf{R}, \hat{\mathbf{n}}) + \beta E_s^{se} \quad (7)$$

where Λ is the de Broglie wavelength of the counterions, $\beta = 1/(k_B T)$, k_B is the Boltzmann constant, T is the absolute temperature, and $\rho(\mathbf{R},\hat{\mathbf{n}})$ is the number density of counterions at position $\mathbf{R}$ and orientation. The short-wavelength contribution to the electrostatic interaction energy $E_s^{se} = 1/2\int d\mathbf{r}\, d\mathbf{r}' \sum(\mathbf{r})G_s(\mathbf{r},\mathbf{r}')\sum(\mathbf{r}')$. The one-body interaction potential of the rod-like molecules $u(\mathbf{R},\hat{\mathbf{n}})$ is defined by

$$u(\mathbf{R}, \hat{\mathbf{n}}) = \sum_{k=0}^{c-1} q_k \int d\mathbf{r}'\, G_s(\mathbf{R} + kl'\hat{\mathbf{n}}, \mathbf{r}') \sum(\mathbf{r}') - \frac{1}{2}\sum_{j,k=0}^{c-1} q_j q_k G_l(\mathbf{R} + jl'\hat{\mathbf{n}}, \mathbf{R} + kl'\hat{\mathbf{n}}) + v(\mathbf{R}, \hat{\mathbf{n}}) \quad (8)$$

where q_k is the charge of site k on the ion and $v(\mathbf{R},\hat{\mathbf{n}})$ is an externally applied potential on the rod-like molecules which is used to prevent them from penetrating the confining plates.

The value of the electric potential $\phi(\mathbf{r}) = \beta^{-1}\mathcal{P}^{-1}i\bar{\psi}_l(\mathbf{r})$ can be found by minimizing the Helmholtz free energy with respect to the long-wavelength field $\delta F/\delta i\bar{\psi}_l(\mathbf{r}) = 0$. The result of minimization procedure is a Poisson equation for the system:

$$-\frac{1}{4\pi}\nabla^2\phi(\mathbf{r}) = \sum(\mathbf{r}) + q(\mathbf{r}) \quad (9)$$

where the charge density of the rods is given by

$$q(\mathbf{r}) = \sum_{k=0}^{c-1} q_k \int d\hat{\mathbf{n}}\, \rho(\mathbf{r} - kl'\hat{\mathbf{n}}, \hat{\mathbf{n}})$$

The density of the counterions is given by

$$\rho(\mathbf{R}, \hat{\mathbf{n}}) = \Lambda^{-3} e^{\beta\mu - \beta u(\mathbf{R},\hat{\mathbf{n}}) - \int d\mathbf{r} Q(\mathbf{r}-\mathbf{R},\hat{\mathbf{n}}) i\bar{\psi}_l(\mathbf{r})} \quad (10)$$

where μ is the chemical potential of the counterions. This is a constant that is determined from the electroneutrality of the system.

From the solution of this integral-differential equation, we can obtain the electric potential ϕ. The value of the parameter σ in the operator $\mathcal{P}$ is determined by the condition

$$\frac{\partial F}{\partial \sigma} = 0 \quad (11)$$

The results depend on the precise value of σ. All static properties of the system can be calculated from the approximate free energy functional (i.e., eq 7).

3. SIMULATION DETAILS

Monte Carlo (MC) simulations were performed for a systems of uranyl ions confined between two parallel walls with identical, uniform surface charges. The charge on two walls exactly compensated the total net charge of uranyl ions to preserve the electroneutrality of the system. The simulations were performed using the integrated Monte Carlo/molecular dynamics/Brownian dynamics simulation suite MOLSIM.[44]

Since the MC simulations cannot be performed for point charges, all ions were modeled as charged hard spheres; the radius of uranium was 0.05 nm, and the radius of oxygen was 0.025 nm. Consequently, small but inevitable differences in the density profiles in the vicinity of charged walls between the theory for point charges and the simulation results arose due to the finite ionic radii. Periodic boundary conditions in the x and y directions were applied to minimize boundary effects. The electrostatic energy was calculated using minimum image method, as thoroughly described by eqs 16–18 in ref 45.

The uranyl ions were initially placed randomly in the simulation box. Each trial move consists of both random displacement and random rotation. The displacement parameters were chosen to obtain ca. 50% acceptance rate. Each simulation consisted of an equilibration run of 50×10^3

attempted moves per particle, followed by a production run of 200×10^3 attempted moves.

To calculate single particle distributions, the z axis was divided into bins. The standard deviation of values in histograms was less than 0.5% for each separate bin in all cases.

4. RESULTS AND DISCUSSION

We investigate a system of uranyl ions confined between two plates with surface charge densities of $\Sigma = 0.05$, 0.1, and 0.2 C m^{-2}. These systems range from the weak coupling to the intermediate coupling regimes. The density distribution of the center of the uranyl ions is plotted in Figure 2 for various plate

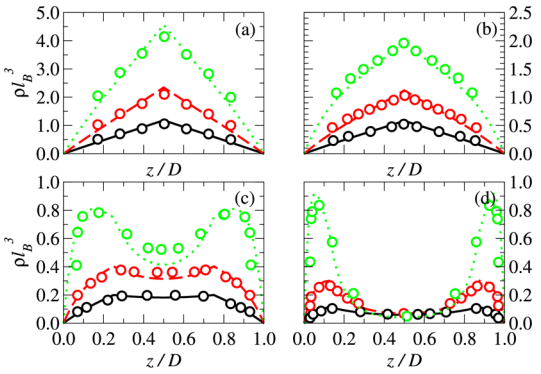

Figure 2. Density profile of uranyl ions confined between plates, with surface charge density $\Sigma = 0.05$ (black), 0.1 (red), and 0.2 C m^{-2} (green), separated by a distance (a) $D = l/2 = 0.18$ nm, (b) $D = l = 0.36$ nm, (c) $D = 2l = 0.72$ nm, and (d) $D = 4l = 1.44$ nm. The lines are the predictions of the splitting theory, and the symbols are from Monte Carlo simulation.

spacings. The symbols are the results of Monte Carlo simulations, and the lines are the predictions of the splitting theory described in previous section. At large plate separations, the ion density profiles peak near the charged surfaces; however, the maximum of the density distribution is not located directly at the charged surfaces, due to the loss of orientation configurations of the uranyl ions as a consequence of excluded volume interactions and to the repulsion between the surface charge and the charge of the oxygen sites.

At plate separations that are comparable to or closer than the length of the uranyl ion, the density profile peaks midway between the plates. The peaks from the left and right plates at larger plate separations merge in the center into one pronounced peak for plate separations comparable to the length of uranyl ion.

Overall, there is good agreement between the predictions of the theory and the Monte Carlo simulation data for all surface charges, from the weak coupling through to the strong coupling regimes. Note that the mean-field approximation works well only at low surface charge densities, while the strong coupling expansion works only at very large surface charge densities.

The theory works well at both short and large plate separations. Deviations of the theory and simulation results at short plate separations is due mainly to the addition of excluded volume interactions in the simulation model. The greatest deviations between the theory and the simulation results are at intermediate plate separations. Similar results are found with the theory for point charge counterions.[46] The results of the splitting theory can be improved by including the next order cumulant correction to the short-wavelength fluctuations of the electrostatic potential;[46] this is equivalent of incorporating the second order virial term in the short-ranged electrostatic interactions.

The distribution of the counterion charge is shown in Figure 3. The charge density profiles are qualitatively similar in shape

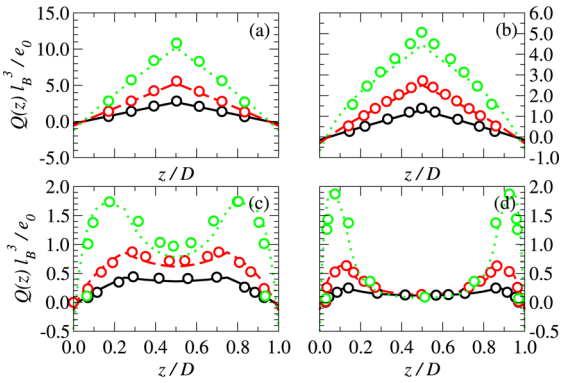

Figure 3. Charge distribution of uranyl ions confined between plates, with surface charge density $\Sigma = 0.05$ (black), 0.1 (red), and 0.2 C m^{-2} (green), separated by a distance (a) $D = l/2 = 0.18$ nm, (b) $D = l = 0.36$ nm, (c) $D = 2l = 0.72$ nm, and (d) $D = 4l = 1.44$ nm. The lines are predictions of the splitting theory, and the symbols are results of MC simulation.

to the density distributions of the uranyl ions. Near the surface of the plate, there is a net negative charge (the same sign as the charge of the plates). This is due to the entropic exclusion of the center of the uranyl ion from the plate surface. The effect is more pronounced for larger surface charge densities.

In Figure 4, we plot the integral of the charge density from the uranyl ions from the left plate. Note that the total

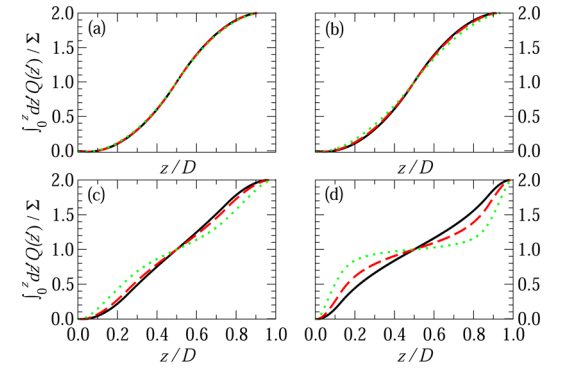

Figure 4. Integrated charge distribution of the uranyl ions confined between plates, with surface charge density $\Sigma = 0.05$ (black), 0.1 (red), and 0.2 C m^{-2} (green), separated by a distance (a) $D = l/2 = 0.18$ nm, (b) $D = l = 0.36$ nm, (c) $D = 2l = 0.72$ nm, and (d) $D = 4l = 1.44$ nm.

integrated charge density should equal -2Σ, because the charge of the uranyl ions should exactly neutralize the surface charge densities of the plates.

The orientation of the uranyl ions is characterized by the order parameter:

$$S(z) = \int_{-1}^{1} \mathrm{d}\cos\theta \left(\frac{3}{2}\cos\theta - \frac{1}{2}\right)\rho(z, \cos\theta) \qquad (12)$$

where θ is the angle between the axis of the uranyl ion and a vector perpendicular to the plates. If the ions are perfectly perpendicular to the plates, then $S = 1$. If the ions are

dx.doi.org/10.1021/jp404822f | J. Phys. Chem. B 2013, 117, 10846−10851

completely aligned parallel to the plates, then $S = -1/2$. If the ions are randomly oriented, then $S = 0$. We plot the local orientational order parameter for the uranyl ions in Figure 5.

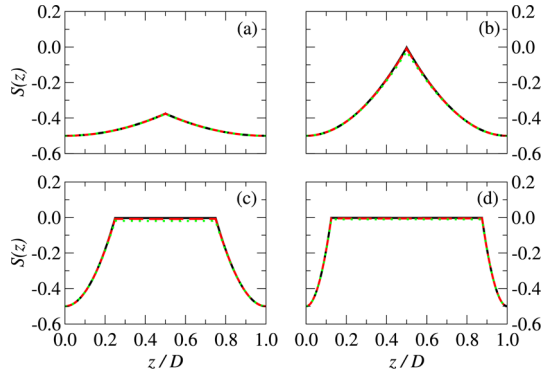

Figure 5. Orientational order parameter of uranyl ions confined between plates, with surface charge density $\Sigma = 0.05$ (black), 0.1 (red), and 0.2 C m^{-2} (green), separated by a distance (a) $D = l/2 = 0.18$ nm, (b) $D = l = 0.36$ nm, (c) $D = 2l = 0.72$ nm, and (d) $D = 4l = 1.44$ nm.

Near the surface of the plates, the uranyl ions align themselves parallel to the plates. At a distance greater than $l/2 = 0.18$ nm from the plate, the ions become randomly orientated. When the plates are closely spaced $(D < l)$, the ions are forced to remain aligned with the plates. Note that there is no bridging effect for these systems because ends of the uranyl ions have a similar charge to that on the plates.

This fact is in close agreement with the results obtained from atomistic simulations.[7] There is a general tendency for uranyl ions to be parallel to the surface. In the case of inner-sphere complexes, this orientation is related to the bond between the uranyl atoms and the ones of the surfaces. In the case of outer-sphere complexes, there is also a similar tendency, and there is no necessity to consider complex specific atomistic bonds, since simple continuous solvent models also predict the same tendency.

In Figure 6, we plot the variation of the pressure between two charged plates with their spacing. The solid lines are for systems where uranyl ions are confined between the plates, and the dashed lines are for point divalent counterions. All the systems have the same qualitative behavior, with a repulsive interaction between the plates at short distances and at long

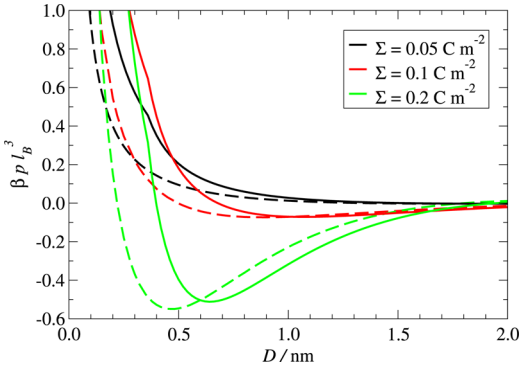

Figure 6. Pressure between two charged plates with intervening counterions, where the charge density of the plates is (i) $\Sigma = 0.05$ (black), (ii) 0.1 (red), and (iii) 0.2 C m^{-1} (green). The solid lines are for uranyl ions, and the dashed lines are for point divalent ions.

distances. At intermediate plate spacings, the plates are attracted to each other. As the plate surface charge density decreases, the attractive region shifts to larger distances and the strength of the attraction decreases and eventually vanishes.

At small spacings, the plates with uranyl ions have a stronger repulsion between them than for the point divalent ions. However at large distances, the systems with uranyl ions have a greater attraction than for the point divalent ions. For larger surface charge densities, the attraction between like charged surfaces appears at plate spacings which roughly correspond to the length of uranyl ions. At large distances, the systems with uranyl ions have a greater attraction than those with point divalent ions. The reason is the spatial charge extension within particular uranyl ion.

Thus despite their orientational order, uranyl ions appear to be unable to induce effective forces between surfaces following the mechanism proposed by Marcelja and Radic.[47] In the case of water, uranyl ions are associated to a larger order next to the surfaces than in the bulk, but it is not enough to induce an attractive hydration force. The model we presented is valid only when the molecular nature of the solvent and the surface can be neglected. This assumption breaks down when specific complexation/hydration forces occur.[48] Namely, the solute mediated ion−ion interactions give rise to ion specific effects.[49−51] In that case, this short-range forces has to be added to the model.

In the recycling process, the spherical structures made of organic molecules enable the separation of the uranyl ions from aqueous solution. The uranyl ions are small compared to the radii of spherical structures and the curvature of the surfaces can be neglected. The system can be described as planar. The force between like charged surfaces can control the geometry of the system. This force can be influenced mainly by surface charge density, as shown from the numerical results shown in Figure 6.

5. CONCLUSIONS

In summary, we have used an approximate field theory to analyze the behavior of rod-like uranyl ions confined between two interacting, like-charged, planar surfaces. This field theory is known to provide accurate predictions for multivalent rod-like ions composed of point charges that are spaced in a linear arrangement.

The resulting theory was applied to uranyl ions, which can be considered as rod-like molecular ions with a spatially distributed charge. The uranyl ions were embedded in a system of like charged surfaces. We performed Monte Carlo simulations for these systems in order to validate the predictions of the theory. This field theory is able to accurately reproduce the results from Monte Carlo simulations.

We examined the influence of surface charge density and surface separation on the concentration profile of uranyl ions. We showed that away from the surfaces, the uranyl ions have no orientational order. However, near the charged surfaces the uranyl ions are preferentially aligned with the surfaces, due to excluded volume interactions. Due to the restriction of the orientational degrees of freedom, the density of ions at the charged surface decreases to zero. This is especially important for separation chemistry because the complexation effects for which uranyl ions are parallel to the surface are especially favorable.

Further we considered the influence of surface charge density on the pressure between like charged surfaces. For large surface

dx.doi.org/10.1021/jp404822f | J. Phys. Chem. B 2013, 117, 10846−10851

charge densities, the force between like charged surfaces becomes attractive, as a result of charge correlations. As the surface charge density decreases, the attractive region moves to larger distances. The strength of the attraction decreases and eventually becomes repulsive. At short and long distances between the surfaces, we obtained a repulsive interaction. At intermediate surface spacings, the plates are attracted to each other. In this system, there is no bridging mechanism where the rod-like uranyl ions span the two plates, as the ends of the uranyl ions have the same charge as the surface. Ion correlations are found to be important, and they can lead to an attraction between the surfaces.

The predictions made in this work may be verified experimentally by measuring the force between like charged surfaces. This type of experiments would provide new insights for the study of interactions between like charged surfaces mediated by uranyl ions.

AUTHOR INFORMATION

Notes

The authors declare no competing financial interest.

ACKNOWLEDGMENTS

Financial support of K.B., J.R., and J.F.D. from CEA through Grant Q1-0005 is acknowledged. J.R. thanks the Slovenian Research Agency for support through Grant P1-0201.

REFERENCES

(1) Ye, X.; Cui, S.; de Almeida, V. F.; Hay, B. P.; Khomami, B. *Phys. Chem. Chem. Phys.* **2010**, *12*, 15406−15409.
(2) Guilbaud, P.; Wipff, G. *J. Phys. Chem.* **1993**, *97*, 5685−5692.
(3) Greathouse, J.; Cygan, R. *Phys. Chem. Chem. Phys.* **2005**, *7*, 3580−3586.
(4) Baaden, M.; Schurhammer, R.; Wipff, G. *J. Phys. Chem. B* **2002**, *106*, 434−441.
(5) Jayasinghe, M.; Beck, T. L. *J. Phys. Chem. B* **2009**, *113*, 11662−11671.
(6) Buhl, M.; Kabrede, H.; Diss, R.; Wipff, G. *J. Am. Chem. Soc.* **2006**, *128*, 6357−6368.
(7) Geckeis, H.; Lutzenkirchen, J.; Polly, R.; Rabung, T.; Schmidt, M. *Chem. Rev.* **2013**, *113*, 1016.
(8) Auwer, C. D.; Drot, R.; Simoni, E.; Conradson, S.; Gailhanou, M.; de Leon, J. M. *New. J. Chem.* **2003**, *27*, 648.
(9) Kremleva, A.; Kruger, S.; Rosch, N. *Langmuir* **2008**, *24*, 9515.
(10) Kremleva, A.; Kruger, S.; Rosch, N. *Geochim. Cosmochim.* **2011**, *75*, 706.
(11) Zaidan, O.; Greathouse, J.; Pabalan, R. *Clays Clay Miner.* **2003**, *51*, 372.
(12) Greathouse, J.; Cygan, R. *Environ. Sci. Technol.* **2006**, *40*, 3865.
(13) Hiemstra, T.; Venema, P.; van Riemsdijk, W. *J. Colloid Interface Sci.* **1989**, *133*, 91.
(14) Hiemstra, T.; Venema, P.; van Riemsdijk, W. *J. Colloid Interface Sci.* **1996**, *184*, 680.
(15) Kallay, N.; Zalac, S. *J. Colloid Interface Sci.* **2000**, *230*, 1−11.
(16) Bohinc, K.; Iglič, A.; May, S. *Europhys. Lett.* **2004**, *68*, 494−500.
(17) May, S.; Iglič, A.; Reščič, J.; Maset, S.; Bohinc, K. *J. Phys. Chem. B* **2008**, *112*, 1685−1692.
(18) Maset, S.; Reščič, J.; May, S.; Pavlič, J. I.; Bohinc, K. *J. Phys. A* **2009**, *42*, 105401.
(19) Teif, V. B.; Bohinc, K. *Prog. Biophys. Mol. Biol.* **2011**, *105*, 208−222.
(20) Grime, M. A.; B., K.; Khan, M. O. *Langmuir* **2010**, *26*, 6343.
(21) Kim, Y. W.; Yi, J.; Pincus, P. A. *Phys. Rev. Lett.* **2008**, *101*, 208305.
(22) Bohinc, K.; Reščič, J.; Maset, S.; May, S. *J. Chem. Phys.* **2011**, *134*, 074111.
(23) Bohinc, K.; Grime, J. M. A.; Lue, L. *Soft Matter* **2012**, *8*, 5679−5686.
(24) Urbanija, J.; Bohinc, K.; Bellen, A.; Maset, S.; Iglič, A.; Kralj-Iglič, V.; Kumar, P. B. S. *J. Chem. Phys.* **2008**, *129*, 105101.
(25) Ibarra-Armenta, J. G.; Martin-Molina, A.; Bohinc, K.; Quesada-Prez, M. *J. Chem. Phys.* **2012**, *137*, 224701.
(26) May, S.; Bohinc, K. *Croatica Chem. Acta* **2011**, *84*, 251−257.
(27) Kirkwood, J. G.; Shumaker, J. B. *Proc. Natl. Acad. Sci. U.S.A.* **1953**, *38*, 863−871.
(28) Kjellander, R.; Marčelja, S.; Pashley, R. M.; Quirk, J. P. *J. Phys. Chem.* **1988**, *92*, 6489−6492.
(29) Moreira, A. G.; Netz, R. R. *Phys. Rev. Lett.* **2001**, *87*, 078301.
(30) Levin, Y. *Rep. Prog. Phys.* **2002**, *65*, 1577−1632.
(31) Shklovskii, B. I. *Phys. Rev. E* **1999**, *60*, 5802−5811.
(32) Coalson, R.; Duncan, A. *J. Chem. Phys.* **1992**, *97*, 5653−5661.
(33) Coalson, R.; Walsh, A.; Duncan, A.; Bental, N. *J. Chem. Phys.* **1995**, *102*, 4584−4594.
(34) Tsonchev, S.; Coalson, R.; Duncan, A. *Phys. Rev. E* **1999**, *60*, 4257−4267.
(35) Tsonchev, S.; Coalson, R. D.; Duncan, A. *Phys. Rev. E* **2007**, *76*, 041804.
(36) Hatlo, M. M.; Lue, L. *Soft Matter* **2009**, *5*, 125−133.
(37) Hatlo, M. M.; Karatrantos, A.; Lue, L. *Phys. Rev. E* **2009**, *80*, 061107.
(38) Hatlo, M. M.; Lue, L. *EPL* **2010**, *89*, 25002.
(39) Hatlo, M. M.; Bohinc, K.; Lue, L. *J. Chem. Phys.* **2010**, *132*, 114102.
(40) Bohinc, K.; Lue, L. *Chin. J. Polymer Sci.* **2011**, *29*, 414−420.
(41) Bohinc, K.; Grime, J. M. A.; Lue, L. *Soft Matter* **2012**, *8*, 5679−5686.
(42) Stratonovich, R. L. *Dokl. Akad. Nauk SSSR* **1957**, *115*, 1097−1100.
(43) Hubbard, J. *Phys. Rev. Lett.* **1959**, *3*, 77−78.
(44) Linse, P. MOLSIM, Version 4.1.7; Lund University: Sweden, 2006.
(45) Jönsson, B.; Wennerström, H.; Halle, B. *J. Phys. Chem.* **1980**, *84*, 2179−2185.
(46) Hatlo, M. M.; Banerjee, P.; Forsman, J.; Lue, L. *J. Chem. Phys.* **2012**, *137*, 064115.
(47) Marčelja, S.; Radic, N. *Chem. Phys. Lett.* **1976**, *42*, 129.
(48) Molina, J. J.; Lectez, S.; Tazi, S.; Salanne, M.; Dufrêche, J.-F.; Roques, J.; Simoni, E.; Madden, P. A.; Turq, P. *J. Chem. Phys.* **2011**, *134*, 014511.
(49) Boström, M.; Lima, E.; Biscaia Jr., E.; Tavares, F.; Kunz, W. In *Specific Ion Effects*; Kunz, W., Ed.; World Scentific: Singapore, 2010; Chapter 11, pp 293−310.
(50) Kunz, W.; Neueder, R. In *Specific Ion Effects*; Kunz, W., Ed.; World Scentific: Singapore, 2010; Chapter 1, pp 3−54.
(51) Bohinc, K.; Shrestha, A.; Brumen, M.; May, S. *Phys. Rev. E* **2012**, *85*, 031130.